International Conference on Space Optics—ICSO 2014

La Caleta, Tenerife, Canary Islands

7–10 October 2014

SWIR HgCdTe avalanche photiode focal plane array performances evaluation

E. de Borniol

J. Rothman

F. Salveti

P. Feautrier

SWIR HgCdTe AVALANCHE PHOTIODE FOCAL PLANE ARRAY PERFORMANCES EVALUATION

E. de Borniol[1], J. Rothman[1], F. Salveti[2], P. Feautrier[3].
[1]Univ. Grenoble Alpes, CEA, LETI, MINATEC campus, 38054 Grenoble, France.
[2] Sofradir, BP21, 38113 Veurey-voroize, France.
[3] IPAG, BP 53, 38041 Grenoble Cedex 9, France.

I.   INTRODUCTION

One of the main challenges of modern astronomical instruments like adaptive optics (AO) systems or fringe trackers is to deal with the very low photons flux detection scenarios. The typical timescale of atmospheric turbulences being in the range of some tens of milliseconds, infrared wavefront sensors for AO systems needs frame rates higher than 1 KHz leading to integration times lower than 1 ms. This integration time associated with a low irradiance results in a few number of integrated photons per frame per pixel. To preserve the information coming from this weak signal, the focal plane array (FPA) has to present a low read out noise, a high quantum efficiency and a low dark current. Up to now, the output noise of high speed near infrared sensors is limited by the silicon read out circuit noise. The use of HgCdTe avalanche photodiodes with high gain at moderate reverse bias and low excess noise seems then a logical way to reduce the impact of the read noise on images signal to noise ratio. These low irradiance passive imaging applications with integration times in the millisecond range needs low photodiode dark current and low background current. These requirements lead to the choice of the photodiode cut off wavelength. The short wave infrared (SWIR) around 3 µm is a good compromise between the gain that can be obtain for a given APD bias and the background and dark current. The CEA LETI HgCdTe APD technology, and a fine analysis of the gain curve characteristic are presented in [1] and won't be detailed here. The response time of the APD is also a key factor for a high frame rate FPA. This parameter has been evaluated in [2] and the results shows cut off frequencies in the GHz range.

In this communication we report the performances of a SWIR APD FPA designed and fabricated by CEA LETI and SOFRADIR for astrophysical applications. This development was made in the frame of RAPID, a 4 years R&D project funded by the French FUI (Fond Unique Interministériel). This project involves industrial and academic partners from the field of advanced infrared focal plane arrays fabrication (SOFRADIR and CEA LETI) and of astronomical/defense institutes (IPAG, LAM, ONERA). The goal of this program is to develop a fast and low noise SWIR camera for astronomical fast applications like adaptive optics wavefront sensing and fringe tracking for astronomical interferometers [3].

The first batch of FPA's was based on liquid-phase epitaxy (LPE) grown photodiode arrays with 3 µm cut off wavelength. In order to get higher avalanche gain for a given photodiode reverse bias voltage, we have made a second batch with a cadmium composition leading to 3.3 µm cut off wavelength (λ_c). This paper described the read out circuit in the next section. The aim section III is to find the critical parameter that has to be measured to evaluate the signal to noise ratio (SNR) of an APD FPA. The main electro optical characteristics of an FPA based on 3.3µm cut off wavelength APDs are reported in "Rapid FPAs characterisation" section. The dark current evolution with temperature of a 3 µm FPA high and low APD bias is also detailed in this section.

II.   READ OUT CIRCUIT DESIGN

The read out circuit (ROIC) developed for the RAPID project consist in a 320 by 256 pixels array with 30µm pitch. The input stage uses a capacitive trans-impedance amplifier (CTIA) to get a good linearity and an intra-pixel correlated double sampling (CDS) to reach low read out noise levels. The CDS signal is memorized in each pixel allowing an integration while read (IWR) signal output and so an integration time using almost all the frame period. With 8 analog video output the RAPID ROIC reaches a frame rate of 2 KHz at 20 MHz pixel clock. The conception goal was to get less than 2 electrons of input referred read noise at 80 K.
The key ROIC design parameters are listed in Table 1.

Table 1 : Rapid ROIC specifications

RAPID ROIC	
Parameter	Specification
Operating temperature	80 K
Format	320 x 256
Pixel pitch	30 µm
Maximum frame rate	2 KHz
Input stage	CTIA + CDS
Integration mode	Snapshot
Read out mode	Integration while read
Input referred noise	2 electron at gain 20

III.   SIGNAL TO NOISE RATIO ANALYSIS

The aim of the following analysis is to point out the APD FPA measurable parameter allowing to evaluate the SNR of each pixel of an FPA for any given number of photon per pixel. This SNR evaluation needs the knowledge of the excess noise due to the gain noise and the quantum efficiency of the APD. The evaluation of these two parameters in our particular case is detailed here after. This analysis assumes a linear APD mode and is valuable for more than 1 photon per integration time.

A. Excess noise factor and QEFR

During the characterization of a SWIR RAPID FPAs, we have observed some devices exhibiting a mean value of the measured excess noise factor (F_{meas}) value below 1. As an example a value 0,94 was measured for the 3.3µm cut off wavelength device. The F definition detailed later implies that a F value below 1 is not physic. A difference between the true F and the measured value has ever been observed by DRS [4]. The origin of this difference was explained by a variation of the pixel fill factor when the photodiode is biased. In our case an F_{meas} below 1 suggest that the fill factor slightly increases when the APD is biased. The pixel QE can be defined as the ratio between the number of incoming photons to the number of electrons collected by the photodiode before multiplication by the gain. From this simple definition, a fill factor increase will lead to a QE increase. This QE evolution has two main consequences that will be detailed in the following analysis.

The APD gain is usually measured by the ratio between high and low bias signals. If the QE slightly increases when the photodiode is biased to get the gain, the measured gain G_{meas} will contain both the true gain G and QE variation and gives an over-estimation of the gain. If Q_1 is the quantum efficiency low APD bias (at unity gain) and Q the QE at high bias, the only equation that can be written is:

$$G_{meas} = \frac{Q}{Q_1} G \qquad (1)$$

The second consequence of QE variation with the bias is that the excess noise factor measurement can result in a value lower than the theoretical low limit of 1. F is defined as the ratio of SNR at the input of the APD to the SNR at the output. Here we are using the photonic F, the ratio between SNR limited by the photon noise before APD gain, $SNR_{SN\,In}$ to the value of this SNR after gain, $SNR_{SN\,Out}$

$$F = \frac{SNR_{SN\,In}}{SNR_{SN\,Out}} \qquad (2)$$

For a given number of integrated photons N_{ph}, the shot noise limited SNR before APD gain is:

$$SNR_{SN\,In} = QN_{ph} \qquad (3)$$

and so:

$$F = \frac{QN_{ph}}{SNR_{SN\,Out}} \qquad (4)$$

As Q is unknown, the SNR before the APD gain can't be evaluated from (3).

The input shot noise limited SNR that can be measured is:

$$SNR_{SN\,In\,meas} = Q_1 N_{ph} \qquad (5)$$

F_{meas} being defined as the value of F evaluated from $SNR_{SN\ In\ Meas}$ and the measurement of SNR with the APD biased, $SNR_{SN\ Out\ Meas}$, then we get:

$$F_{meas} = Q_1 N_{ph}/SNR_{SN\ Out\ meas} \tag{6}$$

And making the ratio with (4):

$$F_{meas} = \frac{Q_1}{Q} F \tag{7}$$

It's now clear that F_{meas} is underestimated when the QE increase with APD bias. Even if the true values of Q and F can't be measured, the Q/F ratio or QEFR is accessible to the measure via the following relation simply deducted from the previous one:

$$QEFR = Q_1/F_{meas} \tag{8}$$

B. Noise equivalent number of photons and signal to noise ratio

The evaluation of the SNR that will provide an APD based FPA for a given number of incoming photons is crucial for all kind of applications. Another useful parameter is the number of photon producing a signal equal to the total noise of the FPA. For the following calculation, we will assume a negligible background flux. To avoid confusion with other formulation of the noise equivalent number photon taking into account the noise of the signal itself [5], we will name this one the dark noise equivalent number of photons and use the notation N_{deph}.

From a noise measurement in dark condition, we get an evaluation of the sum of the dark current and the read noise. If we name this total dark noise at the output of the APD σ_{dark} and from the previous the N_{deph} is:

$$N_{deph} = \sigma_{dark}/(GQ) \tag{9}$$

Using (1), we get a formulation using parameters accessible to measurement:

$$N_{deph} = \sigma_{dark}/(Q_1 G_{meas}) \tag{10}$$

Readout circuit noise of APD based FPA are often expressed in electrons back referred to the photodiode input (i.e. before APD gain). When the QE changes with bias, we don't have access to the true gain and the back referred FPA noise expressed in electron is unknown. The FPA noise can only be expressed in Volt at the output of the FPA or in photons at the input of the photodiode.

The SNR at the output of the FPA is:

$$SNR_{Out} = \frac{S_{Out}^2}{\sigma_{SN\ Out}^2 + \sigma_{dark}^2} \tag{11}$$

S_{Out} being the FPA output photonic signal expressed in electron and $\sigma_{SN\ Out}$ the photonic shot noise in electron. By expressing the signal and noise of (4), it comes:

$$\sigma_{SN\ Out}^2 = FG^2 Q N_{ph} \tag{12}$$

And then (11) gives:

$$SNR_{Out} = QEFR \frac{N_{ph}^2}{N_{ph} + \sigma_{dark}^2/FG^2Q} \tag{13}$$

The product FG²Q can be expressed from measurable FPA parameters. It's the ratio $Q_1^2 G_{meas}^2/QEFR$.

$$SNR_{Out} = \frac{N_{ph}^2}{N_{ph}/QEFR + (\sigma_{dark}/Q_1 G_{meas})^2} \tag{14}$$

$$SNR_{Out} = \frac{N_{ph}^2}{N_{ph}/QEFR + N_{deph}^2} \tag{15}$$

This SNR formulation allows to evaluate the SNR at the output of the FPA for any number of incoming photons and from measureable figures of merit: the QEFR and N_{deph}. This is also valuable when the QE is stable with APD bias, but as we have seen before, if it's not the case, some precautions have to be taken to evaluate QEFR and N_{deph}.

IV.   RAPID FPAs CHARACTERISATION

The following electro optic measurements and figures of merit concern the same FPA based on a 3.3 µm APD array and were made at a FPA temperature of 80 K. The study of current in dark conditions that was made for another device with 3 µm cut off wavelength.

A. Conversion capacitance evaluation

The conversion capacitance is calculated from the slope of the total current of the array as a function of the mean output voltage of all pixels. As for other photonic measurements, the FPA is in front of an extended black body and equipped with an f/4.1 cold screen.The current variation was obtain by changing the temperature of a black body in front of the FPA from 15°C to 30°C. A conversion capacitance C_{int} of 4.14 fF was determined from Fig. 1 for a low APD bias voltage (unity gain). For higher bias, the gain, QE and C_{int} evaluations can't be distinguished.
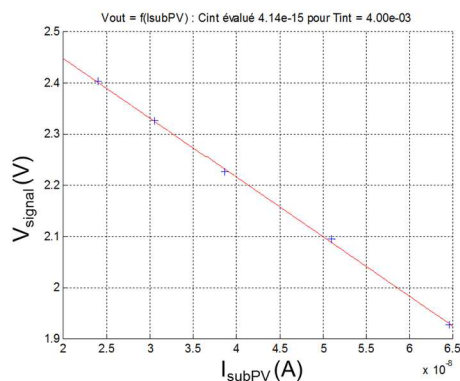

Fig. 1 : RAPID FPA integration capacitance evaluation at low APD bias voltage (-0.2 V).

B. Electro optical FPA performances measurements and experimental SNR evaluation

The gain was measured from the FPA response to a black body temperature (T_{bb}) variation of 5°C around 17.5 C. The use of the response method avoids any confusion between the dark current and the gain as it can be when measuring the gain from a simple current ratio. For the 3.3 µm cut off FPA, a mean value gain of 31 is obtained at 8 Volt of reverse bias. The pixel to pixel or spatial standard deviation is quite low at 2.2. More important than the gain dispersion is the uniformity of an image after non uniformity correction (NUC). As an example, we have simply make a NUC from two images at different integration times (30 µs and 80 µs) at 8 Volt of APD reverse bias. Fig. 2 is the result of the NUC applied to an image at a third integration time of 60 µs. The 82 bad pixels deviates by more than 33 % of the mean value. The Y scale limits of the image are also fixed at more or less 33 % of the mean value. The residual fixed pattern noise (RFPN) in this case is less than 2.8 % of the mean value. This good uniformity after NUC is preserved when the photon flux on the FPA changes. Fig. 3 shows a flat field in front of a 20°C black body with the NUC recorded at 15°C used for Fig. 2. The spatial dispersion is very low at 1.3% and there is only 39 bad pixels.
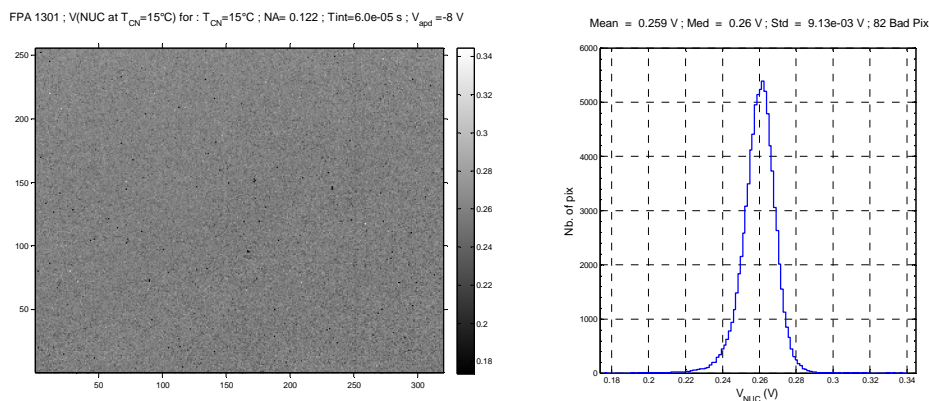

Fig. 2 : T_{bb} = 15°C flat field map and histogram for 8 Volt of APD reverse bias (measured gain of 31) after non uniformity correction.

FPA 1301 ; V(NUC at T$_{CN}$=20°C) for : T$_{CN}$=15°C ; NA= 0.122 ; Tint=6.0e-05 s ; V$_{apd}$ =-8 V   Mean = 0.44 V ; Med = 0.44 V ; Std = 5.79e-03 V ; 39 Bad Pix

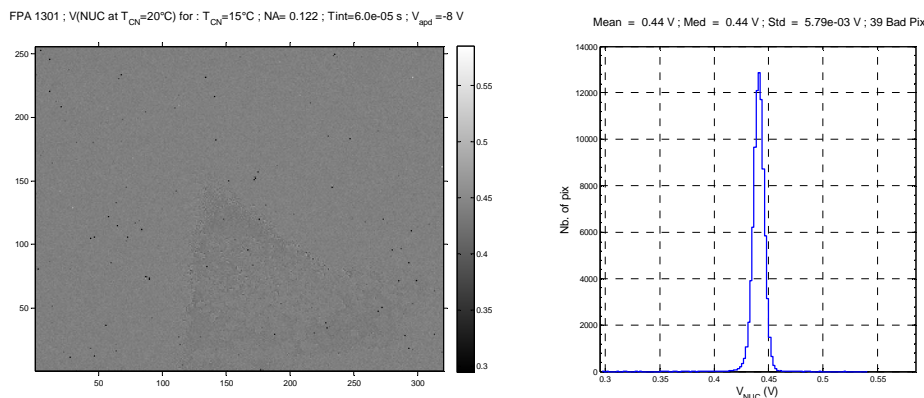**Fig. 3 :** T$_{bb}$ = 20°C flat field histogram for 8 Volt of reverse bias (measured Gain of 31) after non uniformity correction with a NUC performed at 15°C.

As it was done for the gain, the quantum efficiency is evaluated by changing the black body temperature and making the ratio between the calculated variation of the number of photons per pixel and the variation of integrated electrons. By working on difference we eliminate a possible background photonic signal. As we don't use any optical filter, the calculation of the number of incoming photons is made from the measured spectral response of a photodiode coming from the same LPE-grown wafer than the APD pixels.

For F evaluation, we use an expression obtained from (7) and (12):

$$F_{meas} = \frac{\sigma^2_{SN\,Out}}{G^2_{meas}Q_1 N_{ph}} \qquad (16)$$

Using (1) e and the expression of the FPA output signal and noise voltages, $V_{Out} = \frac{q}{C_{int}} GQN_{ph}$ and

$\sigma^2_{Vout\,meas} = \left(\frac{q}{C_{int}}\right)^2 \sigma^2_{SN\,Out}$, we obtain a simple expression of F$_{meas}$:

$$F_{meas} = \frac{\sigma^2_{Vout\,meas}}{G_{meas}\frac{qV_{Out}}{Cint}} \qquad (17)$$

Output voltage and noise values used for F calculation are the difference between short and long integration time measurements in order to eliminate the circuit offset and read noise. The mean excess noise measured at -8 Volt (gain 31) is 0.94. For this APD geometry configuration the quantum efficiency increases with photodiode bias.

The noise in the dark was measured at 600 µs integration time in a passively cooled cryostat designed for very low residual photon flux. This integration time allows a frame rate of 1.5 KHz representative of the typical value needed for AO. Given the weak dark current measured at 80 K, the noise in the dark is dominated by the ROIC noise.

The QEFR and N$_{deph}$ maps evaluated from the previous gain, F, QE and noise in dark conditions measurements are presented Fig. 4. The QEFR shows a mean value of 0.59 with a weak spatial dispersion of 1.7 %. This dispersion only takes into account the QE dispersion at low APD bias as we use the mean value of F_{meas} for the QEFR evaluation. A mean N$_{deph}$ of less than 3 photons is obtained. We can observe a tail for high values side of the N$_{deph}$ histogram. The read out circuit is highly suspect to be the source of these noisy pixels. Indeed, most of them are common to low and high APD reverse bias voltage noise measurements. Furthermore, we have also observe this tail for a short integration time in all FPA tested. We have now identify the most probable source of excess noise in the ROIC. A new design and conception would clearly improve the ROIC noise performance.
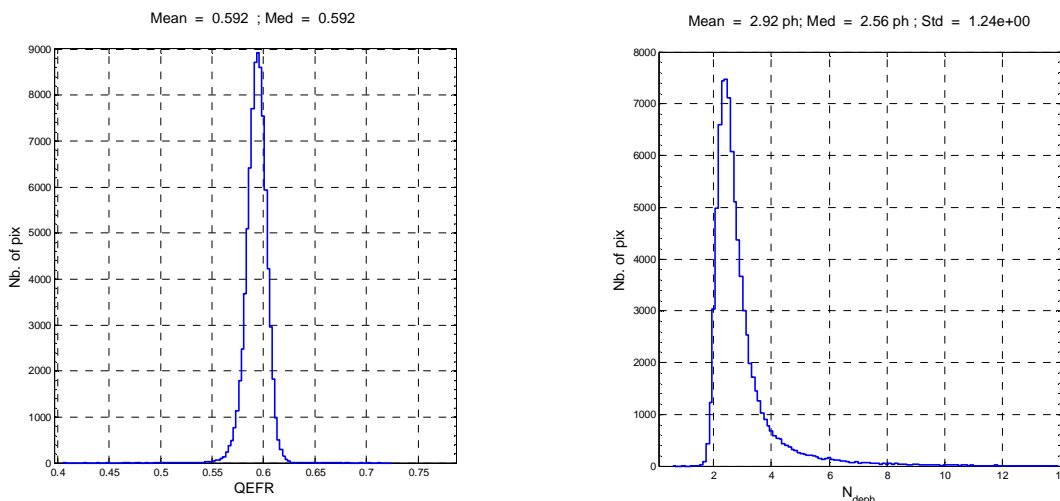
Mean = 0.592 ; Med = 0.592

Mean = 2.92 ph; Med = 2.56 ph ; Std = 1.24e+00

Fig. 4 : QEFR and N_{deph} histograms of the 3.3 µm cut off FPA at -8V (G_{meas} = 31).

For imaging applications at low signal level, it may be convenient to express SNR in amplitude rather than in power. The previous SNR_{Out} was expressed from the power definition in order to stay coherent with classical F definition. The SNR in amplitude (SNR_{Amp}) is given by the square root of (15). The evolution of SNR_{Amp} with the number of photons per pixel and per frame for the tested FPA is plotted Fig. 5. The shot noise limited SNR and the SNR that can be evaluated at unity gain from the dark noise and QE measurement are also plotted.

An histogram of SNR_{Amp} for 20 photons per frame per pixel evaluated from QEFR and N_{deph} maps is also depicted in Fig. 6. The mean SNR_{Amp} of 3 is coherent with the value obtained from the curve of Fig. 5. From these curves we can also notice a FPA output SNR under 1.5 without gain and a shot noise limited value of 3.3. The noise histogram displays a noise tail coming from dark noise and then as we said before, probably from the ROIC. The noise histogram curve becomes much more symmetric when photonic noise overcomes this excessive read out noise (Fig. 7). This is a good indication that noisy pixels observed in dark measurements are not due to avalanche photodiodes with excessive F.
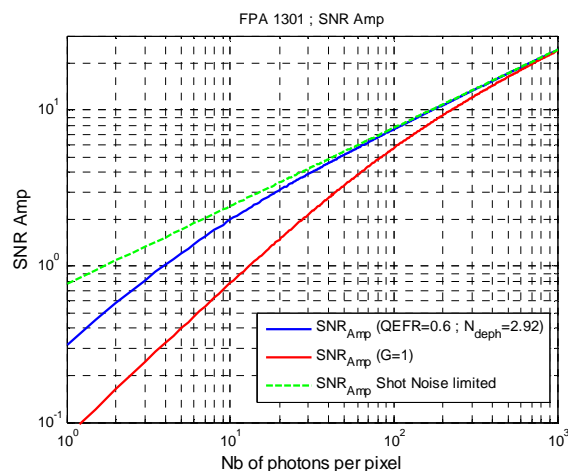
FPA 1301 ; SNR Amp

Fig. 5 : SNR_{Amp} for the 3.3 µm cut off FPA calculated from the mean QEFR and N_{deph} measured values at -8V (blue curve). The red curve is evaluated for the same FPA without APD gain (with the measured dark noise unity gain).
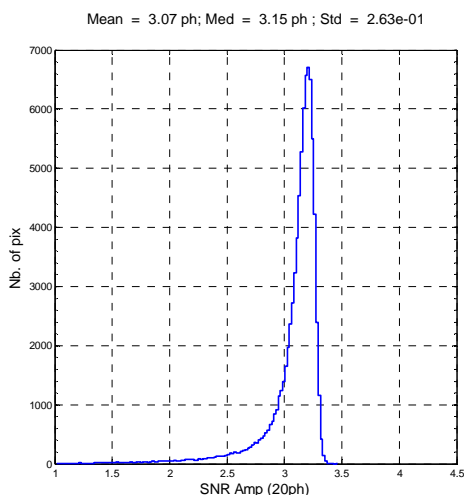
Mean = 3.07 ph; Med = 3.15 ph ; Std = 2.63e-01

Mean = 26.9 e-; Med = 26.8 e- ; Std = 2.30e+00

Fig. 6 : example of calculated SNR_{Amp} histogram of the 3.3 µm cut off FPA from the QEFR and N_{deph} maps at -8 V and assuming a signal of 20 photons per pixel per frame.
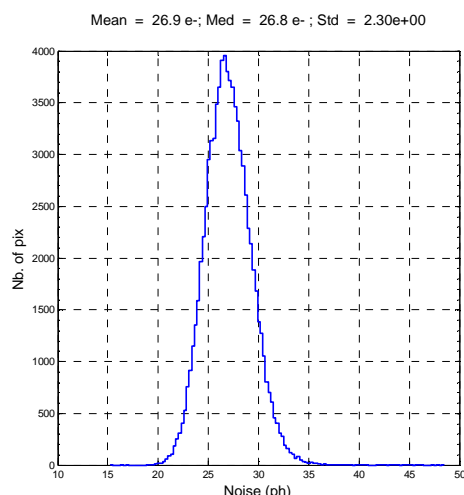
Fig. 7 : Back referred measured noise histogram of the 3.3 µm cut off FPA under illumination expressed in photons (divided by Q_1G_{meas}) at -8 V, 30 µs integration time and TCN = 15°C.

C. Dark current of a 3 µm FPA

The RAPID FPAs have been used to measure the 3µm APD dark current evolution with temperature between 80 K and 200 K. The aim of these measurement was to get information about the limiting diode current process.

The mean dark current density of a 3µm FPA was measured at high and low APD reverse bias (Fig. 8). Currents values are normalized by the pixel area, $(30 \text{ µm})^2$, and by the measured gain for the high reverse bias. For both measurements we have also plotted a fit using the sum of a generation recombination (GR), a diffusion and a photonic current. Indeed we have observed a saturation in the decrease of the current with temperature at the same level for both APD bias. As the Si ROIC was not optimized to reduce the electroluminescence we believe that this limitation at 1×10^{-12} A/cm^2 (or 56 e-/s/pixel) current comes from the circuit glow. This current value was used as photonic current to fit the experimental data. For this manual fit of our data, we have used the same value of diffusion current at low and high APD bias. At low bias, the GR current like contribution exceeds the diffusion like current under 150 K. For the same device biased at -6.3 V (gain of 7.3) the GR dominates above 180 K. If the current at high bias would follow the GR trend, the pixel dark current would reach 2.4×10^{-15} A/cm^2 or 0.13 e-/s for our 30 µm pixel.

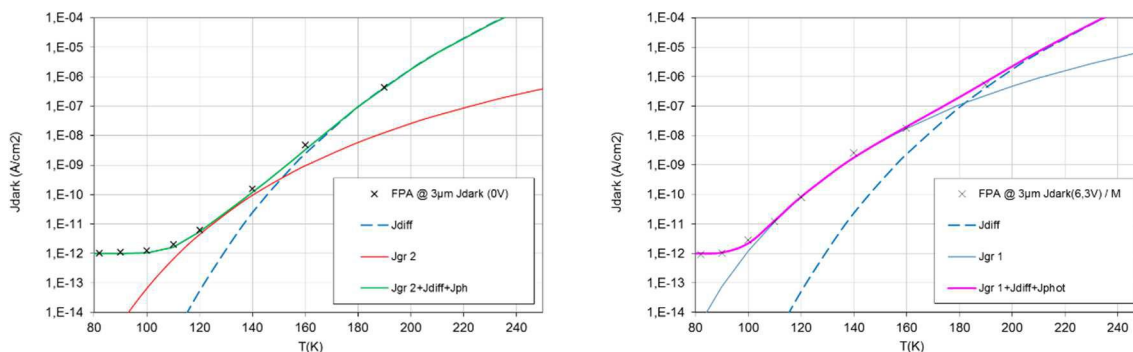**Fig. 8 :** 3 µm cut off wavelength APD FPA current measurement in dark conditions at -0.2 V (left) and -6.3 V (right) reverse bias.

V.   CONCLUSION

CEA LETI and SOFRADIR have develop HgCdTe APD detectors for astrophysics applications like AO and fringe tracking. The electro optical characterisations performed on the detectors have demonstrated that the initial FPA performance specifications have been fulfilled. During the test we have observed some devices with a measured excess noise factor slightly lower than 1. This can be explained by a slight increase of the QE when the APD is biased to get gain. In that case, the true values of the gain and excess noise factors are not directly accessible to the measure. But we have shown that even in that case, the global output SNR can be evaluated from two figures of merit accessible to measurement: the QEFR and the dark noise equivalent number of photon.

For a 3.3 µm cut off wavelength FPA with a mean gain of 31 at -8 V of APD bias we have measured a mean QEFR of 0.6 and a N_{deph} of 2.9 photons. The SNR have been evaluated from these experimental values using the formulation obtained by our analysis. As an example, a mean amplitude signal to noise ratio of 3.1 is expected for 20 photons per pixel for this FPA not that far from the shot noise limited value of 3.3. Without gain, the expected FPA SNR value evaluated from measurement of the dark noise and QE would be 1.5. Noise in the dark measurement have revealed a non-negligible number of pixels presenting an excessive noise. This excessive noise is attributed to the ROIC. The origin of the noise is probably identified and new design would greatly improve this unexpected CMOS behavior.

The RAPID ROIC has been used to evaluate the dark current of a 3µm cut off wavelength APD array. Under a 100 K we observed a current limited by the ROIC electroluminescence equivalent to 56 e-/s for a 30 µm pixel. Between 100 K and 180 K, the dark current divided by the photonic measured gain shows a GR behavior with increasing temperature. Without ROIC glow, if we extrapolate the GR trend under 100 K the dark current would reach 2.4×10^{-15} A/cm^2 or 0.13 e-/s for a 30 µm pixel.

REFERENCES

[1] J. Rothman, L. Mollard, S. Bosson, G. Vojetta, K. Foubert, S. Gatti, G. Bonnouvrier, F. Salveti, A. Kerlain, and O. Pacaud, "Short-Wave Infrared HgCdTe Avalanche Photodiodes," *J. Electron. Mater.*, vol. 41, no. 10, pp. 2928–2936, Oct. 2012.

[2] J. Rothman, K. Foubert, G. Lasfargues, and C. Largeron, "Response Time Measurements in Short-Wave Infrared HgCdTe e-APDs," *J. Electron. Mater.*, vol. 43, no. 8, pp. 2947–2954, Aug. 2014.

[3] P. Feautrier, J.-L. Gach, M. Downing, P. Jorden, J. Kolb, J. Rothman, T. Fusco, P. Balard, E. Stadler, C. Guillaume, and others, "Advances in detector technologies for visible and infrared wavefront sensing," in *SPIE Astronomical Telescopes+ Instrumentation*, 2012, p. 84470Q–84470Q.

[4] J. Beck, M. Woodall, R. Scritchfield, M. Ohlson, L. Wood, P. Mitra, and J. Robinson, "Gated IR Imaging with 128 × 128 HgCdTe Electron Avalanche Photodiode FPA," *J. Electron. Mater.*, vol. 37, no. 9, pp. 1334–1343, Sep. 2008.

[5] G. Finger, I. Baker, and R. Dorn, "Development of high-speed, low-noise NIR HgCdTe Avalanche Photodiode Array for Adaptative Optics and Interferometry," 2010.